

1. TITLE
2. INVESTIGATOR(S)
3. INTRODUCTION
4. THEORY OF ALGORITHM/MEASUREMENTS
5. EQUIPMENT
6. PROCEDURE
7. OBSERVATIONS
8. DATA DESCRIPTION
9. DATA MANIPULATIONS
10. ERRORS
11. NOTES
12. REFERENCES
13. DATA ACCESS
14. GLOSSARY OF ACRONYMS

1. TITLE

1.1 Data Set Identification

Subsets extracted from Global Inventory Modeling and Mapping Studies (GIMMS) Satellite Drift Corrected and NOAA-16 Incorporated Normalized Difference Vegetation Index (NDVI), Bi-monthly, 1981–2003.

1.2 Database and Database Table Name(s)

Not applicable to this data set.

1.3 File Name(s)

The files in this data set are named using the following naming convention:

CC_name_num.ext

where

CC

is one of the following continent codes

AF = Africa

AZ = Australia and New Zealand

EA = Eurasia

NA = North America

SA = South America and Central America

and

name

is the DAAC core site name of the subset

num

is an arbitrary site number

ext

is the file suffix, where **img** refers to the data cube file type, and **hdr** refers to the associated ENVI ascii header file

Each file contains 540 bi-monthly maximum-value composite NDVI image bands, from July 1, 1981 to December 31, 2003. There are two images, or bands, per month. The names designated in the header file with an `a` are the subsets for the first half of the month, and the `b` designator refers to the subsets for the second half of the month. The images are 25 lines by 25 pixels in dimension, and are geolocated in the accompanying ENVI header file.

1.4 Revision Date of this Document

September 24, 2004.

2. INVESTIGATOR(S)

2.1 Investigator's Name and Title

Jorge E. Pinzon and Molly E. Brown
 Science Systems and Applications
 NASA-Goddard Space Flight Center
 Code 923
 Greenbelt, MD 20771

Compton J. Tucker
 NASA-Goddard Space Flight Center
 Code 923
 Greenbelt, MD 20771

2.2 Title of Investigation

Monitoring Seasonal and interannual variations in Land-Surface Vegetation from 1981-2003 using GIMMS NDVI.

2.3 Contacts (For Data Production Information)

	Contact 1	Contact 2
2.3.1 Name	Dr. Jorge E. Pinzon	Dr. Molly E. Brown
2.3.2 Address	NASA-Goddard Space Flight Center Code 923 Greenbelt, MD 20771 USA	NASA-Goddard Space Flight Center Code 923 Greenbelt, MD 20771 USA
2.3.3 Tel. No.	301-614-6685	301-614-6616
Fax No.	301-614-6015	301-614-6015
2.3.4 E-mail	jorge_pinzon@ssaihq.com	molly.brown@gsfc.nasa.gov

2.4 Requested Form of Acknowledgment

*Global Inventory Modeling and Mapping Studies (GIMMS) AVHRR 8km
 Normalized Difference Vegetation Index (NDVI), Bimonthly 1981–2003.*

Please cite the following publications whenever these data are used:

- Pinzon, J., M. E. Brown and C. J. Tucker. 2004. Satellite time series correction of orbital drift artifacts using empirical mode decomposition. In Hilbert-Huang Transform: Introduction and Applications, eds. N. Huang, pp. Chapter 10, Part II. Applications (to appear).
- Pinzon, J. 2002. Using HHT to successfully uncouple seasonal and interannual components in remotely sensed data. SCI 2002. Conference Proceedings Jul 14-18. Orlando, Florida.
- Tucker, C. J., J. E. Pinzon, M. E. Brown, D. Slayback, E. W. Pak, R. Mahoney, E. Vermote and N. El Saleous. 2005. An Extended AVHRR 8-km NDVI Data Set Compatible with MODIS and SPOT Vegetation NDVI Data. International Journal of Remote Sensing (submitted).

3.0 INTRODUCTION

3.1 Objective/Purpose

The Global Inventory Modeling and Mapping Studies (GIMMS) normalized difference vegetation index (NDVI) data sets were generated to provide a 22-year satellite record of monthly changes in terrestrial vegetation. New features of this dataset include reduced NDVI variations arising from calibration, view geometry, volcanic aerosols, and other effects not related to actual vegetation change. In particular, NOAA-9 descending node data from September 1994 to January 1995, volcanic stratospheric aerosol correction for 1982-1984 and 1991-1994, and improved NDVI using empirical mode decomposition/reconstruction (EMD) to minimize effects of orbital drift. Global NDVI was generated to provide inputs for computing the time series of biophysical parameters contained in the International Satellite Land Surface Climatology Project (ISLSCP) Initiative II collection. NDVI is used in climate models and biogeochemical models to calculate photosynthesis, the exchange of CO₂ between the atmosphere and the land surface, land-surface evapotranspiration and the absorption and release of energy by the land surface.

3.2 Summary of Parameters

Composited, bi-monthly, normalized difference vegetation index over global land area subsets. NDVI is the difference (in reflectance) between the AVHRR near-infrared and visible bands divided by the sum of these two bands (Tucker 1980; Sellers 1985; Sellers et al. 1994).

3.3 Discussion

Because NDVI is a ratio of differences between two adjacent bands, it is largely *insensitive* to variations in illumination intensity. However, NDVI *is sensitive* to effects that differ between bands. Band calibrations, for example, have changed frequently between the five NOAA AVHRR instruments that acquired the NDVI record for the 22-year Initiative II period. In addition, natural variability in atmospheric aerosols and column water vapor affect the NDVI record. Over the period of record two major volcanic eruptions occurred, El Chichon in 1982 and Mt. Pinatubo in 1991, injecting large quantities of aerosols into the Earth's stratosphere. These

*Global Inventory Modeling and Mapping Studies (GIMMS) AVHRR 8km
Normalized Difference Vegetation Index (NDVI), Bimonthly 1981–2003.*

aerosols, along with smoke from biomass burning and dust from soil erosion and other factors, can introduce significant variability in the AVHRR NDVI record. These constituents have significantly different effects on AVHRR band's 1 and 2. The GIMMS NDVI corrects for the known changes of the atmosphere from these two volcanic eruptions, but reductions in the NDVI signal can still be seen over densely vegetated tropical land covers for limited time periods.

NDVI is also sensitive to the periodic variations in solar illumination angle and sensor view angles induced by the NOAA orbits. Its polar, sun-synchronous orbits permitted daily coverage of each point on earth, although at time-varying viewing and illumination geometry. The GIMMS NDVI dataset has a satellite overpass time drift correction that largely eliminates the variation of NDVI due to changes in solar zenith angle.

Frequent cloud cover can also create numerous gaps in the daily AVHRR record eliminating roughly two-thirds of the data. In order to construct cloud-free views of the Earth, *composite* images were constructed at regular intervals by selecting pixels with the maximum NDVI. Choosing pixels with maximum NDVI reduces cloud cover and water vapor effects since both strongly reduce NDVI. Image compositing can be done over any time interval, but 9-10 days is generally the minimum period selected for maximum quality. The GIMMS data record constructed here is based on 15-day composites. There are two 15-day composites per month, the first for days 1-15, and the second for day 16 to the end of the month.

4. THEORY OF ALGORITHM/MEASUREMENTS

Green leaves have a higher reflectance in the AVHRR near-infrared band (band 2) than in the visible band (band 1), because of differences in leaf chlorophyll absorption between the two bands. Chlorophyll absorbs strongly in the red region, spanned by AVHRR band 1. Thus, the difference in vegetation reflectance between the near-infrared and visible bands increases with green leaf vegetation density, hence chlorophyll concentration. The ratio of the difference between band 2 and band 1 and their sum, hence the NDVI, is an index that ranges between -1 and +1, though the observed range is usually smaller. Non-vegetated materials generally have a much lower NDVI (near 0) than dense vegetation (~0.7), since their reflectance in the near-infrared and visible bands are more nearly equal.

5. EQUIPMENT

5.1 Instrument Description

The Advanced Very High Resolution Radiometer (AVHRR) acquired data in 5 spectral bands; one visible, one near infrared and three thermal bands, all with 1024 quantizing levels. The thermal bands are not used in the GIMMS NDVI data. The AVHRR produces imagery at 1.1 and 4 km spatial resolution. The 4-km product or global area coverage (GAC) product is derived from the 1-km product by onboard sampling. The 4-km product is available globally from July 1981 until the present. The 1-km record is not continuous. Its availability depends upon prior arrangements made by NOAA, or on the proximity of a local receiving station that can capture

Global Inventory Modeling and Mapping Studies (GIMMS) AVHRR 8km Normalized Difference Vegetation Index (NDVI), Bimonthly 1981–2003.

the data directly from the satellite. See NOAA–KLM users guide for specifications of the newest NOAA AVHRR instruments. <http://www2.ncdc.noaa.gov/docs/klm/>

5.1.1 Platform

The NOAA AVHRR satellite series 7, 9, 11, 14 and 16, used for this NDVI record, flew in sun-synchronous polar orbits with a nominal 1:30 or 2:30 PM local daytime overpass time at launch. However, the overpass times drifted by 1-2 minutes per month to as much as 4 1/2 hours later in the day, creating variable illumination and view angles over the period of record. The 55-degree sensor swath width permitted a daily view of each pixel on Earth, although at different illumination and view angles during the 9-day repeat cycle. Maximum-value NDVI data compositing tends to select pixels acquired in a near-nadir mode with minimum atmospheric effects. Even so, view, illumination and atmospheric effects remain. Reducing these effects was the aim of the GIMMS processing.

The satellite platforms the data are derived from are noted below:

Table 1. Instrument change times for the GIMMS dataset.

AVHRR instrument	Start date	End date
NOAA-7	July 1, 1981	February 8, 1985
NOAA-9	February 11, 1985	November 7, 1988
NOAA-11	November 11, 1988	September 19, 1994
NOAA-9 (descending)	September 20, 1994	January 18, 1995
NOAA-14	January 19, 1995	October 31, 2000
NOAA-16	November 1, 2000	December 31, 2003
NOAA-17	January 1, 2004	continuing

5.1.2 Mission Objectives

The NOAA AVHRR satellite sensor series was originally designed as a weather satellite. However from the early 1980s, AVHRR data has found increasing use to monitor the type and condition of land vegetation. AVHRR vegetation data archives extend back to August 1981.

5.1.3 Key Variables

The AVHRR measured top of the atmosphere radiance in 5 bands. Band 1 covered the 0.5 to 0.7 um region, band 2 the 0.7 to 1.1 um region, with three thermal bands one covering the middle infrared region around 3 microns and two thermal infrared bands in the 10 to 11 micron region. The GIMMS NDVI product uses radiance in bands 1 and 2 and were mapped at the NASA Goddard Space Flight Center under the guidance of Dr. Compton Tucker. The current adjusted NDVI dataset was derived entirely from the NDVI produced during the 1998-2000 remapping effort of the GIMMS group.

5.1.4 Principles of Operation

The NOAA satellite series, NOAA 6, 7, 9, 11 and 14 were in polar, sun-synchronous orbits with nadir afternoon overpass times. NOAA 7 data span the years 1981 -1985, NOAA 9, 1986-1989, NOAA 11, 1989-1995, NOAA 14, 1995-2000, and NOAA-16 from 2000 to 2004 (and continues through the present). Data from NOAA-9 was used from September 1994 until January 1995 when NOAA 11 started to malfunction and its replacement, NOAA 13, failed shortly after launch. Each AVHRR sensor has different and variable calibration and overpass time.

5.1.5 Instrument Measurement Geometry

The AVHRR is a scanning, imaging radiometer, scanning ± 55 degrees, providing a 2800 km swath width. The orbital configuration permits daily coverage at a maximum spatial resolution of 1 km of each point on earth, although at different viewing and illumination geometries on subsequent days. The orbit repeats its ground track each 9 days.

5.1.6 Manufacturer of Instrument

See NOAA–KLM users guide for specifications of the newest NOAA AVHRR instrument. <http://www2.ncdc.noaa.gov/docs/klm/>

5.2 Calibration

NOAA provides preflight calibration coefficients that relate the satellite-measured digital counts to reflectance values. The preflight calibration coefficients for the visible and near infrared channel are of the form

$$\text{reflectance} = \text{gain} * (\text{digital counts} - \text{offset})$$

The gain and the offset are determined on the ground prior to launch of the satellite; The gain and offset are referred to as pre-flight calibration coefficients. The preflight calibration coefficients change for each satellite. In some cases preflight coefficients were updated during the time of operation of a satellite.

Pre-flight calibration coefficients do not take into account the degradation of the AVHRR during its time of operation. Several techniques exist to correct for the change in sensitivity of the AVHRR. For the GIMMS data, the coefficients by Vermote and Kaufman (1995) are used to correct the visible and near infrared reflectance for in-flight sensor degradation. In the GIMMS NDVI data the relative degradation error in the gain is further reduced to below 1 % by using a desert calibration of the ratio of channels 1 and 2 reflectance to invariant Sahara Desert targets.

5.2.1 Specifications

5.2.1.1 Tolerance

See Vermote and Kaufman (1995) and Section 9.2.1 for more details.

5.2.2 Frequency of Calibration

Global Inventory Modeling and Mapping Studies (GIMMS) AVHRR 8km Normalized Difference Vegetation Index (NDVI), Bimonthly 1981–2003.

See Vermote and Kaufman (1995) and Section 9.2.1 for more details. (Vermote and Kaufman 1995)

5.2.3 Other Calibration Information

See Rao and Chen (1995). (Rao and Chen 1995)

6. PROCEDURE

6.1 Data Acquisition Methods

The input data for the GIMMS Land data processing is the NOAA AVHRR GAC 1B data. Our GAC 1B data were obtained from NOAA and from NCAR sources at the time of acquisition from 1985 to the present. We have augmented this dataset with GAC 1B data available from NOAA's Satellite Active Archive. The GIMMS NDVI datasets were corrected using solar zenith angle values from the AVHRR sensor for the period of 1981-2003 (Pinzon 2002; Pinzon et al. 2004; Tucker et al. 2005).

6.2 Spatial Characteristics

6.2.1 Spatial Coverage

- Before subset extraction, the coverage is global for all land areas except Greenland and Antarctica. Data in the files are ordered from North to south and from West to East beginning at 180 degrees West longitude and 90 degrees North latitude.

6.2.2 Spatial Resolution

The data are provided at an 8 km pixel spatial scale.

6.3 Temporal Characteristics

6.3.1 Temporal Coverage

The data are available from July 1981 through December 31, 2003. North American and African subsets may contain extractions through May of 2004.

6.3.2 Temporal Resolution

Bi-monthly; the GIMMS dataset is composited at a nominal 15-day time step.

7. OBSERVATIONS

7.1 Field Notes

Not applicable to this dataset.

8. DATA DESCRIPTION

Global Inventory Modeling and Mapping Studies (GIMMS) AVHRR 8km Normalized Difference Vegetation Index (NDVI), Bimonthly 1981–2003.

8.1 Table Definition with Comments

Not applicable to this dataset.

8.2 Type of Data

8.2.1 Parameter/ Variable Name

GIMMS Normalized Difference Vegetation Index, corrected for (see section 9.2.2 for details):

- residual sensor degradation and sensor intercalibration differences;
- distortions caused by persistent cloud cover globally;
- solar zenith angle and viewing angle effects due to satellite drift;
- volcanic aerosols;
- missing data in the Northern Hemisphere during winter using interpolation due to high solar zenith angles;
- low signal to noise ratios due to sub-pixel cloud contamination and water vapor.

8.2.2 Parameter/ Variable Description

NDVI is archived in signed 16-bit band-sequential integer files of the entire period of record for each site. The image flags have been imbedded into the one's place in the integer values. Good NDVI values are four digit integers ending in zero, while flagged integers end in non-zero values. In the formulas below, the data, once imported, is referred to as 'raw' data. To recover the -1 to 1 range of NDVI, use the following formula:

$NDVI = raw/10000$ (where the insignificant 4th decimal place can be ignored)

or, to strip off the flag value, use:

$NDVI = (raw/10000)/10$

In the NDVI data,

Water pixels have raw values of -10000

Masked pixels have raw values of -5000

Missing pixels have raw values of -1994

The AVHRR post-processing has improved the quality of the AVHRR NDVI raw data by removing clouds, reducing noise and removing artifacts due to satellite drift. Corrected pixels have been flagged for the user to provide information about what has been done to each pixel. The fourth decimal place in NDVI can be ignored, as it was used for the flags only. Good NDVI values are 'raw' four digit integers ending in zero.

The flag files can be retrieved from the NDVI data by the following formula:

$FLAG = raw - \text{floor}(raw/10) * 10;$

(where FLOOR(X) rounds the elements of X to the nearest integer).

*Global Inventory Modeling and Mapping Studies (GIMMS) AVHRR 8km
Normalized Difference Vegetation Index (NDVI), Bimonthly 1981–2003.*

Thus, users can use the formula to create a mask image of flagged pixels to determine their spatial and frequency distribution as an aid to analysis.

The meaning of the Page 9 of 10FLAG values:

FLAG = 5 (NDVI retrieved from average seasonal profile, possibly snow)

FLAG = 4 (NDVI retrieved from average seasonal profile)

FLAG = 3 (NDVI retrieved from spline interpolation, possibly snow)

FLAG = 2 (NDVI retrieved from spline interpolation)

FLAG = 1 (Good value, possibly snow)

8.2.3 Data Range

NDVI has a theoretical range between -1 and 1; with values around 0 for bare soil (little or no vegetation), and values of 0.7+ for dense vegetation. Raw data range can be from -10000 to 10000.

8.2.4 Units of Measurement

Unitless

8.2.5 Data Source

AVHRR

8.3 Sample Data Record

Not applicable to this dataset.

8.4 Data Format

All of the files in this AVHRR NDVI dataset are in integer format (IEEE standard - big endian). NDVI values are multiplied by 10000, water pixels have a value of -10000, -5000 are masked pixels, and missing are -2000 plus the flag 6.

The files are in the Albers Equal Area Projection. The README file provided has the projection information, as well as a header file appropriate for use with the ENVI software.

8.5 Related Data Sets

The 8 km GIMMS Land Surface AVHRR data set (Tucker et al. 2005) is available at its original spatial resolution directly from the GIMMS group. Please contact Dr. Tucker for this dataset. LAI and FPAR fields at quarter degree resolution based on the GIMMS data are also available.

9. DATA MANIPULATIONS

9.1 Formulas

9.1.1 Derivation Techniques/Algorithms

See Section 9.2.1.

Global Inventory Modeling and Mapping Studies (GIMMS) AVHRR 8km Normalized Difference Vegetation Index (NDVI), Bimonthly 1981–2003.

9.2 Data Processing Sequence

9.2.1 Processing Steps and Data Sets

The original 4.62 km native resolution GAC data has been mapped to 8km in the GIMMS Land Surface AVHRR data set (Tucker et al. 2005). The contents of this dataset are:

- NDVI
- solar zenith angle
- Temperature Channel 4
- Temperature Channel 5

The data set can be obtained from University of Maryland's Global Land Cover Facility (GLCF) and the ISCLCP II initiative web sites.

9.2.2 8-km NDVI Data Processing

Satellite data in NOAA level-1b format (Kidwell 1998) were ingested from magnetic media, were forward mapped to the output bin closest to the center location of each 8 km equal area grid cell, respective calibration values were applied to each channel (Vermote and Kaufman 1995), and the other values associated with the maximum NDVI were retained for each compositing period. Data from seven AVHRR instruments on different satellite platforms were used in this dataset (see Table 1, 5.1.1).

We used a similar navigation procedure to that of El Saleous *et al.* (2000), which in turn is based upon the work of Baldwin and Emery (1995). The orbital model predicts the position of the satellite at any time, using the satellite onboard clock and orbital elements to determine the predicted position. From this perspective, the sun-target-sensor geometry is determined. The NOAA satellites' velocity with respect to the Earth's surface is ~ 7 km/second and the output bin size we employed was 8 km. This translates into a timing error of ~ 1.0 second to achieve a navigation accuracy of less than or equal to 1 pixel. The majority of our navigation errors were due to errors of the onboard spacecraft clock. (El Saleous et al. 2000, Baldwin and Emory 1995)

Every composite image was manually checked for navigation accuracy by comparing the mapped data to a reference coastline for the continent in question. Images with > 1 pixel navigation errors were investigated and the day(s) of the navigation error identified. These images were subsequently reprocessed separately and manually registered to the reference data, to bring the badly navigated day(s) into agreement with the reference coastline. The the composite image was reconstructed by maximum value NDVI compositing. In a few cases it was necessary to discard data from specific days, as the navigation errors were impossible to adjust.

With the failure of NOAA-13 to achieve orbit in 1992, NOAA-11 continued to provide global afternoon/early morning AVHRR data. By 1994, the afternoon equatorial overpass time for NOAA-11 was $\sim 17:00$ hours. We began using NOAA-9 descending node AVHRR data for our global NDVI data set in September 1994, and continued using

these data until NOAA-14 became operational in late January 1995.¹ There is thus a fundamental difference between the Pathfinder AVHRR Land (PAL) and the Global Vegetation Index (GVI) data sets and the data set we describe herein: We use NOAA-9 AVHRR data from October 1994 into January 1995 when there were no NOAA-11 AVHRR data (it had failed), and use NOAA-9 AVHRR data in September 1994 when the PAL and GVI data sets use NOAA-11 data.

9.2.2.1 Radiometric calibration

Satellite determination of long-term surface trends requires precision within and among various space-borne instruments. It is also crucial to document the within- and among-sensor calibration uncertainty to determine the accuracy with which surface trends over time can be ascertained. The NDVI data we describe were processed in two ways: (1) NOAA-7 through NOAA-14 channel 1 and 2 data were processed using the Vermote and Kaufman (1995) channel 1 and channel 2 calibration. The resulting NDVI fields were further adjusted using the desert calibration technique from Los (1998), then decomposed and reconstructed using empirical mode decomposition to correct for solar zenith angle effects (Pinzon 2002); and (2) Data from NOAA-16 were processed using the preflight channel 1 and channel 2 calibration values and formed into maximum values composites. An empirical mode decomposition and reconstruction was performed to insure a slope with respect to time of 0.00 in desert areas, this was also used to correct solar zenith angle artifacts. This NOAA-16 NDVI time series was adjusted by a constant offset to match up with a temporally-coincident and spatially-aggregated 8-km SPOT Vegetation NDVI time series, which had previously been adjusted to match up with the corresponding temporally-coincident NOAA-14 NDVI time series. We thus used overlapping SPOT Vegetation NDVI time series as the means to intercalibrate or tie together the NOAA-14 and NOAA-16 NDVI time series (Pinzon et al. 2004). This was necessary because the bilinear gain for channel 1 and channel 2 of NOAA-16's AVHRR instrument complicates *ex post facto* calibration. Thermal calibration coefficients after Weinreb *et al.* (1990) were used for the calibration of all thermal channels. (Weinreb et al. 1990)

9.2.2.2 Atmospheric Correction and Cloud Screening

We choose to produce a maximum value NDVI composite data set, and associated layers, without any atmospheric correction, except during the El Chichon and Mt. Pinatubo volcanic stratospheric aerosol periods. A stratospheric aerosol correction was applied as proposed by Vermote *et al.* (1997) from April 1982 through December 1984 and from June 1991 through December 1994. We formed composite stratospheric aerosol optical depth fields by combining the work of Sato *et al.* (1993), and Vermote *et al.* (1997). Rosen *et al.* (1994), Russel et al. (1993) and Dutton (1994) were used to compare

¹ NOAA-9 had a daytime descending node equatorial crossing time of ~09:00 hours in mid-1994 to early 1995. It had "rocked around the clock", with a ~2-3 minute/month later time procession from its original day time descending node equatorial crossing time of 02:30 hours.

specific optical depth measurements to our blended global fields. We produced optical depth fields that varied by month and degree of latitude.

Cloud screening was provided by a channel 5 thermal mask of 0° C for all continents except Africa, where a cloud mask of 10° C was used. In addition, the bimonthly composites significantly reduced cloud contamination and the channel 4 and channel 5 thermal values are available for *ex post facto* cloud screening if desired.

9.2.2.3 Satellite drift correction using Pinzon et al (2002) method

The GIMMS group uses Empirical Mode Decomposition (EMD) to identify and remove parts of the NDVI signal that are most related to the satellite drift (Pinzon 2002; Pinzon et al. 2004). The EMD technique was introduced by Nordon Huang in 1998 as an alternative to standard decomposition techniques for representation of nonlinear and non-stationary data that show clear physical scales or frequency content. Unlike Fourier decomposition (Wilks 1995; Trefethen and Bau 1997), the EMD a basis for the signal from the data itself. The EMD is empirical, intuitive, direct, *a posteriori*, and adaptive, with the decomposition functions based on and derived from the data (Huang et al. 1998; Huang et al. 1999). Pinzon et al. (2001) showed that EMD was applicable to NDVI time series from the AVHRR sensor to isolate orbital drift effects from the NDVI signal.(Pinzon et al. 2001)

Orbital drift results in later equatorial crossing times for the NOAA satellites and results in changes of illumination that affect the NDVI. In this dataset, we identify the trends in the NDVI that associated with changes in sun-target-sensor geometry due to satellite drift. Figure 3 shows the effects of satellite drift on the Solar Zenith Angle (SZA) at three latitude bands, 75-35N, 35N-35S and 35S-55S. An increasing trend is observed in each satellite due to its delay in the equatorial crossing time. This trend, superimposed on each plot, is more pronounced at lower latitude, whereas seasonal variations dominate at higher latitudes. Note that equatorial latitudes have an extra oscillation due to solar nadir moving past the target latitude, causing and increase in SZA at six month intervals rather than at yearly intervals (Privette et al. 1995).

The EMD is used to extract NDVI trends that may be caused by the satellite orbital drift, reducing the interference of other components in the NDVI signal. The EMD is used to isolate the components of the NDVI signal that are related to SZA trends and remove them from the corrected NDVI (see Figures 2 and 3). The technique removes NDVI trends that are more than 80% correlated to the SZA trends shown in Figure 2. Areas with trends that have a lower correlation are not corrected. Figure 3 shows both cases: trend removal from NDVI signal due to high correlation with the satellite drift, and trends that have not been altered because of low correlation to satellite drift.

Figure 4 shows areas where the correction is the strongest, notably 1) the tropics are most affected by satellite drift due to the SZA trend magnitudes, and 2) the high northern latitude and regions with low vegetation biomes are less contaminated since the SZA component represents a small part of the NDVI signal (see Figure 2). The correction is performed by-pixel. After the satellite drift correction, a kriging interpolation removes

noise and attenuates the effect of cloudy and missing pixels. The original 8-km AVHRR data is then averaged into 1 degree, 0.5 and 0.25 degree datasets provided here.

9.2.3.4 Intercalibration of NDVI from all instruments using narrow-band instruments such as MODIS and SPOT-Vegetation

In order to include the data from NOAA-16, an intercalibration of the single-gain satellites NOAA-7-14 (historical data) and the dual-gain NOAA-16 with data from SPOT-Vegetation global data at 1 km (Achard et al., 1992). SPOT data was averaged from 1 km to 8 km globally and then decomposed using the EMD method. The interannual trend from three years of data, 20 months overlapping with NOAA-14 and the rest with NOAA-16, was extracted. This trend was determined to be invariant through time over the period examined. A similar trend was extracted from the same period of NOAA-14. A non-linear regression was performed to establish coefficients that transform the historical data into the same range as that of the current and upcoming suite of visible and NIR sensors, such as MODIS, SPOT-Vegetation and others (Morissette et al., 2004). A similar regression was performed for the NOAA-16 data. Once the trends from the historical and NOAA-16 data were transformed into the common range, the data was reconstructed and a consistent time series was established.

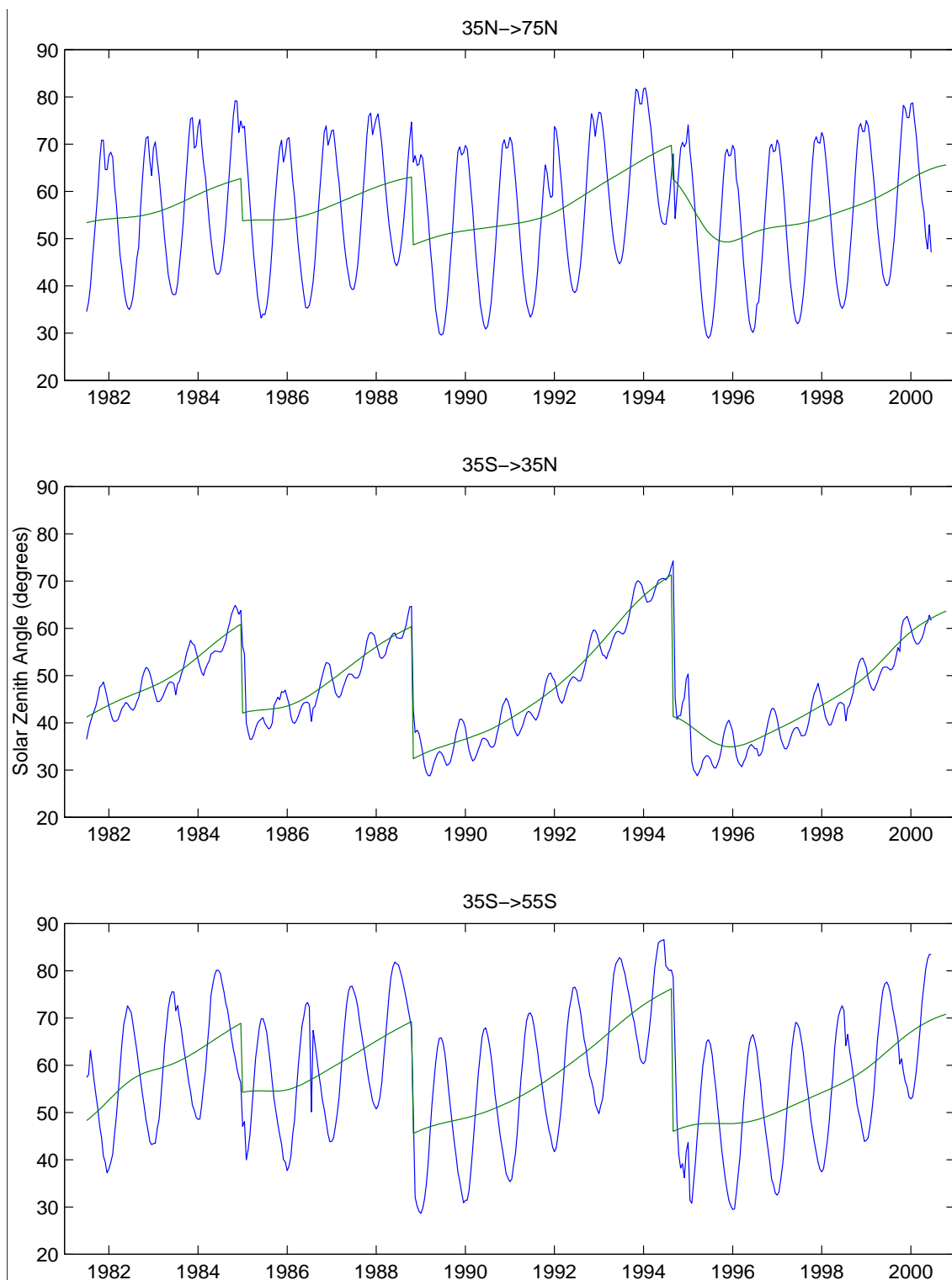


Figure 2. Solar Zenith Angles and trends derived from the NOAA-AVHRR sensor, averaged by latitude bands 75N-35N, 35N-5S, 35S-55S

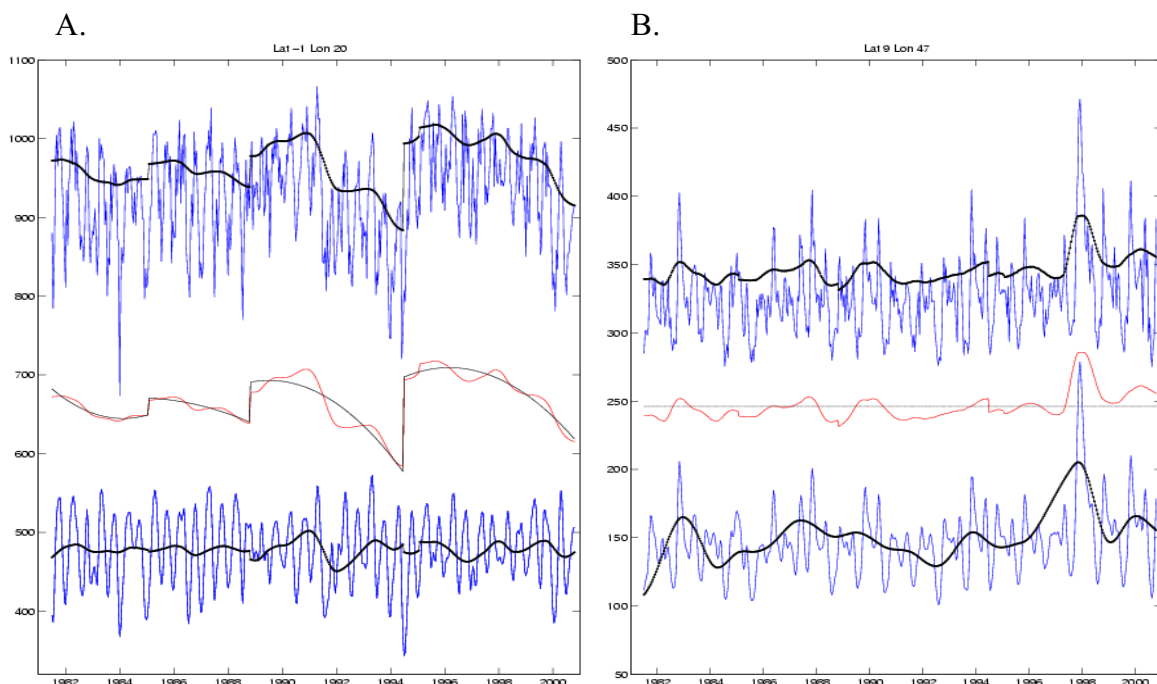


Figure 3. Example of the use of EMD technique and the removal of SZA-correlated trends. A. Before satellite drift correction (series at top), trend removed (middle) and resulting series (bottom). B. A pixel that is not corrected due to lack of correlation with the SZA trends.

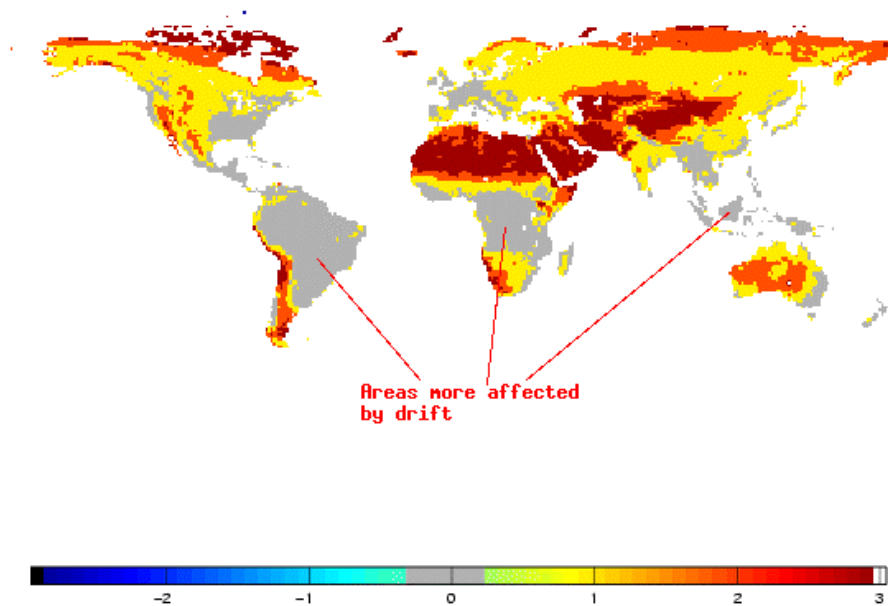


Figure 4. Map displaying continental regions where satellite drift has an important contribution to the signal.

Global Inventory Modeling and Mapping Studies (GIMMS) AVHRR 8km Normalized Difference Vegetation Index (NDVI), Bimonthly 1981–2003.

9.3 Calculations

9.3.1 Special Corrections/Adjustments

None other than those described in 9.1 and 9.2 above.

9.4 Graphs and Plots

See text above, Tucker et al. (2003), Pinzon et al. (2003) for some graphs and plots of the data.

10. ERRORS

10.1 Sources of Error

Some sources of error in the NDVI data set are not accounted for with the GIMMS corrections. These errors are caused by soil background reflectance; this affects low NDVI values, but does not affect high NDVI values. Thus similar low NDVI values may indicate different amounts of vegetation. However, the EMD noise removal diminishes it.

10.2 Quality Assessment

10.2.1 Data Validation by Source

Earlier versions of the GIMMS-NDVI data have been used in various models and seem to capture general patterns of vegetation well. Tests on sites showed reasonable agreement of interannual variation in GIMMS NDVI and other measures of vegetation (Davenport and Nicholson 1993; Malmstrom et al. 1997; D'Arrigo et al. 2000). These tests show that the variation in GIMMS NDVI is realistic on specific sites. Comparison between climate signals and GIMMS NDVI show realistic patterns in many semi-arid regions and temperate regions.

Recent independent research has verified the quality of the NDVI data:

- Lotsch et al (2003a) using the new GIMMS NDVI presented here and global standardized precipitation index (SPI) data revealed geographically extensive patterns of joint NDVI-SPI variability (Lotsch et al. 2003).
- Jia et al (2003) analyzed the GIMMS NDVI data for three bioclimate subzones in northern Alaska and confirmed a long-term trend of increase in vegetation greenness for the Alaskan tundra that has been detected globally for the northern latitudes. There was a 16.9% ($\pm 5.6\%$) increase in peak vegetation greenness across the region that corresponded to simultaneous increases in temperatures (Jia et al. 2003).
- In the Amazon basin, a recent publication by Poveda and Salazar (2004) showed that at interannual timescales, the NDVI shows a reaction to both phases of ENSO. Dryness was seen due to El Nino, whereas NDVI spatial variability is enhanced during La Nina (Poveda and Salazar 2004).
- Lotsch et al (2003b) demonstrated that seasonal GIMMS-NDVI anomalies for Africa, spatial independent component analysis (ICA) reveals coherent regions

that capture high interannual variability in arid and semiarid areas of eastern and southern Africa that were associated with fluctuations in sea surface temperature anomalies (SSTA). When using other AVHRR datasets (here, PAL) known to be contaminated with volcanic aerosols and sensor transition discontinuities, Lotsch et al (2003b) needed to apply ICA correction to account for these artifacts. When using these other datasets, results must be treated with caution (Lotsch et al. 2003).

- Nemani et al (2002) found a 6% increase in NPP using the GIMMS NDVI in their primary production model corresponding with known corresponding with changes in CO₂ concentrations 42% of the increase was from tropical forests due to decreases in cloud cover. Their satellite-based estimates of NPP show significant growth stimulation in both the tropics and the northern high-latitude ecosystems. Assuming that carbon emissions, including those from biomass burning and land-use changes, are properly accounted for in the atmospheric inversions, this spatial discrepancy means that respiration as well as NPP is a major driver of terrestrial carbon-sink dynamics (Nemani et al. 2002).

10.2.2 Confidence Level/Accuracy Judgment

The GIMMS-NDVI data set is believed to give large improvements over the Pathfinder NDVI data set, especially for areas with persistent cloud cover and for needle bearing evergreen vegetation during winter. GIMMS-NDVI has reduced the effects of orbital drift, which are especially large near the end of the time of operation a satellite. Corrections for atmospheric aerosols are likely to be too small from about one to three months after an eruption (May-Jul 1982 for El Chichon and Jul-Sep 1991 for Mt. Pinatubo), where the aerosols have not mixed evenly into the atmosphere (Brown et al. 2003).

10.2.3 Measurement Error for Parameters and Variables

None given.

10.2.4 Additional Quality Assessment Applied

NDVI data are increasingly being used to assess interannual variations in the biosphere; we would like to distinguish between the following types of temporal analysis (Gutman et al. 1995):

- seasonal analysis: NDVI data should have more than sufficient accuracy to assess seasonality of vegetation with great confidence. The one exception may be the small seasonal cycles observed in the Sahara, this seasonality is most likely caused by variations in atmospheric water vapor, not by variations in vegetation.
- interannual analysis: NDVI data have been used to look at year-to-year variations in desert margins (Tucker et al. 1991) and to variations associated with climate oscillations (Myneni et al. 1995). The interannual signal in semi-arid regions and temperate regions is in general larger than the residual errors in the data.

- trend analysis: This is in general the smallest interannual signal in the data; errors in the NDVI data are often as large or larger than the magnitude of trends, at this stage the magnitude of trends in NDVI data is uncertain within an order of magnitude.

11. NOTES

11.1 Known Problems with the Data

The decline in NDVI in mid-1991 was due to the Pinatubo eruption and subsequent cooling and may not be related to actual declines in vegetation. Trends in tropical regions are affected by this decline and should therefore be treated with caution. The high northern latitude (north of 65 degrees) corrections have been made for extremely high solar zenith angles during the winter months, and these values should thus be treated with caution.

11.2 Usage Guidance

GIMMS NDVI presents generalized patterns that may result in poor representations of a specific locale; quantitative conclusions should be drawn with caution. Nevertheless, NDVI should provide a large improvement over previously used NDVI data sets, because the data are collected by one series of instruments, and they give a more realistic representation of the spatial and temporal variability of vegetation patterns over the globe. Users of the data are strongly encouraged to validate their results using independent data.

11.3 Other Relevant Information

Not available at this revision.

12. REFERENCES

12.1 Satellite/Instrument/Data Processing Documentation

Kidwell, K. B. (1998). Polar Orbiter Data Users' Guide (TIROS-N, NOAA-6, NOAA-7, NOAA-8, NOAA-9, NOAA-10, NOAA-11, NOAA-12, NOAA-14), National Oceanic and Atmospheric Administration. <http://www2.ncdc.noaa.gov/docs/podug/>.

Kidwell, K. B. (2000). NOAA KLM User's Guide, National Oceanic and Atmospheric Administration. <http://www2.ncdc.noaa.gov/docs/klm/>.

Pinzon, J., M. E. Brown, et al. (2004). Satellite time series correction of orbital drift artifacts using empirical mode decomposition. Hilbert-Huang Transform: Introduction and Applications. N. Huang: Chapter 10, Part II. Applications.

Tucker, C. J., J. E. Pinzon, et al. (2005). "An Extended AVHRR 8-km NDVI Data Set Compatible with MODIS and SPOT Vegetation NDVI Data." International Journal of Remote Sensing **submitted**.

12.2 Journal Articles and Study Reports.

Achard, F., J.-P. Malingreau, et al. (1992). "A mission for global monitoring of the continental biosphere: the 'Vegetation' Instrument on board SPOT 4." Toulouse, France, LERTS.

Baldwin, D. and W. J. Emory (1995). "Spacecraft altitude variations in NOAA-11 infrared from AVHRR imagery." International Journal of Remote Sensing **16**: 531-548.

Brown, M. E., J. E. Pinzon, et al. (2003). Quantitative Comparison of Four AVHRR Global Data Sets for Land Applications. Greenbelt, MD, Global Mapping and Modelling Systems (GIMMS). **under review**: 35.

D'Arrigo, R. D., C. M. Malmstrom, et al. (2000). "Correlation between maximum latewood density of annual tree rings and NDVI based estimates of forest productivity." International Journal of Remote Sensing **21**(11): 2329-2336.

Davenport, M. L. and S. E. Nicholson (1993). "On the Relation between Rainfall and the Normalized Difference Vegetation Index for Diverse Vegetation Types in East Africa." International Journal of Remote Sensing **14**(12): 2369-2389.

Dutton, E. (1994). 'Aerosol optical depth measurements from four NOAA/CMDL monitoring sites.' Oak Ridge, Tennessee, Carbon Dioxide Information Analysis Center, Oak Ridge National Laboratory: 484-494.

El Saleous, N. Z., E. F. Vermote, et al. (2000). "Improvements in the global biospheric record from the Advanced Very High Resolution Radiometer (AVHRR)." International Journal of Remote Sensing **21**(6-7): 1251-1277.

Emery, W. J., J. Brown, et al. (1989). "AVHRR Image Navigation: Summary and Review." Photogrammetric Engineering and Remote Sensing **55**: 1175-1183.

Gutman, G., D. Tarpley, et al. (1995). "The enhanced NOAA Global land dataset from the Advanced Very High Resolution Radiometer." Bulletin American Meteorological Society **76**(7): 1141-1156.

Huang, N. E., Z. Shen, et al. (1999). "A new view of nonlinear water waves: the Hilbert spectrum." Annual Review of Fluid Mechanics **31**: 417-457.

Huang, N. E., Z. Shen, et al. (1998). "The empirical mode decomposition and the Hilbert spectrum for nonlinear and non-stationary time series analysis." Proceedings of the Royal Society of London **545**: 903-995.

Jia, G. S. J., H. E. Epstein, et al. (2003). "Greening of arctic Alaska, 1981-2001." Geophysical Research Letters **30**(20).

Kidwell, K. B. (1998). "Polar Orbiter Data Users' Guide" (TIROS-N, NOAA-6, NOAA-7, NOAA-8, NOAA-9, NOAA-10, NOAA-11, NOAA-12, NOAA-14). Washington D.C., National Oceanic and Atmospheric Administration.

Global Inventory Modeling and Mapping Studies (GIMMS) AVHRR 8km Normalized Difference Vegetation Index (NDVI), Bimonthly 1981–2003.

- Los, S. O. (1998). "Estimation of the Ratio of Sensor Degradation Between NOAA AVHRR Channels 1 and 2 from Monthly NDVI Composites." IEEE Transactions on Geoscience and Remote Sensing **36**(1): 206-213.
- Lotsch, A., M. A. Friedl, et al. (2003). "Coupled vegetation-precipitation variability observed from satellite and climate records." Geophysical Research Letters **30**(14).
- Lotsch, A., M. A. Friedl, et al. (2003). "Spatio-Temporal Deconvolution of NDVI Image Sequences Using Independent Component Analysis." IEEE Transactions Geoscience and Remote Sensing **41**(12): 2938-2942.
- Malmstrom, C. M., M. V. Thompson, et al. (1997). "Interannual variation in global-scale net primary production: Testing model estimates." Global Biogeochemical Cycles **11**(3): 367-392.
- Morisette, J.T., Pinzon, J.E., Brown, M.E., Tucker, C.J. and Justice, C.O., 2004. "Initial validation of NDVI time series from AVHRR, Vegetation and MODIS." International SPOT 4/5 - VEGETATION users Conference, Antwerp, Belgium.
- Myneni, R. B., F. G. Hall, et al. (1995). "The Interpretation of Spectral Vegetation Indexes." Ieee Transactions on Geoscience and Remote Sensing **33**(2): 481-486.
- Nemani, R., M. White, et al. (2002). "Recent trends in hydrologic balance have enhanced the terrestrial carbon sink in the United States." Geophysical Research Letters **29**(10).
- Pinzon, J. (2002). "Using HHT to successfully uncouple seasonal and interannual components in remotely sensed data." SCI 2002 Conference Proceedings Jul 14-18, Orlando, Florida, SCI International.
- Pinzon, J., M. E. Brown, et al. (2004). "Satellite time series correction of orbital drift artifacts using empirical mode decomposition." Hilbert-Huang Transform: Introduction and Applications. N. Huang: Chapter 10, Part II. Applications.
- Pinzon, J., J. F. Pierce, et al. (2001). "Analysis of Remote Sensing Data Using Hilbert-Huang Transform." SCI 2001 Conference Proceedings.
- Poveda, G. and L. F. Salazar (2004). "Annual and Interannual (ENSO) Variability of Spatial Scaling Properties of a Vegetation Index (NDVI) in Amazonia." Remote Sensing of Environment **in press**.
- Privette, J. L., C. Fowler, et al. (1995). "Effects of Orbital Drift on Advanced Very High Resolution Radiometer Products: Normalized Difference Vegetation Index and Sea Surface Temperature." Remote Sensing of Environment **53**: 164-171.
- Rao, C. R. N. and J. Chen (1995). "Inter-satellite calibration linkages for the visible and near-infrared channels of the Advanced Very High Resolution Radiometer on the NOAA-7, -9, and -11 spacecraft." International Journal of Remote Sensing **16**: 1931-1942.
- Rosen, J. M., N. T. Kjome, et al. (1994). "Decay of Mount Pinatubo aerosol at midlatitudes in the northern and southern hemispheres." Journal of Geophysical Research **99**(D12): 25733-25739.
- Russel, P. B., J. M. Livingston, et al. (1993). "Pinatubo and pre-Pinatubo optical-depth spectra: Mauna Loa measurements, comparisons, inferred particle size distributions, radiative effects, and relationships to lidar data." Journal of Geophysical Research **98**: 22969-22985.

*Global Inventory Modeling and Mapping Studies (GIMMS) AVHRR 8km
Normalized Difference Vegetation Index (NDVI), Bimonthly 1981–2003.*

Sato, M., M. Hansen, et al. (1993). "Stratospheric Aerosol Optical Depths, 1850-1990." Journal of Geophysical Research **98**(D12): 22987-22994.

Sellers, P., C. J. Tucker, et al. (1994). "A global 1 degree x 1 degree NDVI data set for climate studies. Part 2." International Journal of Remote Sensing **15**(17): 3519-3545.

Sellers, P. J. (1985). "Canopy Reflectance, Photosynthesis, and Transpiration." International Journal of Remote Sensing **6**(8): 1335-1372.

Trefethen, L. N. and D. Bau (1997). "Numerical Linear Algebra." Philadelphia, Society for Industrial and Applied Mathematics.

Tucker, C. J. (1980). "Remote Sensing of Leaf Water Content in the Near Infrared." Remote Sensing of Environment **10**: 23-32.

Tucker, C. J., H. E. Dregne, et al. (1991). "Expansion and Contraction of the Sahara Desert from 1980 to 1990." Science **253**: 299-301.

Tucker, C. J., J. E. Pinzon, et al. (2005). "An Extended AVHRR 8-km NDVI Data Set Compatible with MODIS and SPOT Vegetation NDVI Data." International Journal of Remote Sensing **submitted**.

Vermote, E., N. El Saleous, et al. (1997). "Data Pre-Processing: Stratospheric Aerosol Perturbing Effect on the Remote Sensing of Vegetation: Correction Method for the Composite NDVI after the Pinatubo Eruption." Remote Sensing Reviews **15**: 7-21.

Vermote, E. and Y. J. Kaufman (1995). "Absolute calibration of AVHRR visible and near-infrared channels using ocean and cloud views." International Journal of Remote Sensing **16**(13): 2317-2340.

Weinreb, M. P., G. Hamilton, et al. (1990). "Nonlinearity corrections in calibration of Advanced Very High Resolution Radiometer infrared channels." Journal of Geophysical Research **95**: 7381-7388.

Wilks, D. S. (1995). "Statistical Methods in the Atmospheric Sciences, an Introduction." San Diego, Academic Press.

13. DATA ACCESS

13.1 Contacts for Archive/Data Access Information

These subsets are available via the EOS Land Validation web site.

<http://landval.gsfc.nasa.gov/MODIS/>, under the 'Core Sites' link.

The continental NDVI data set from which these data were extracted are available from the University of Maryland's, GLCF (<http://glcf.umiacs.umd.edu/index.shtml>).

The GIMMS Land Surface AVHRR data set (Tucker et al. 2005) can be obtained from the GLCF and the ISCLCP II Initiative web sites.

14. GLOSSARY OF ACRONYMS

AVHRR	Advanced Very High Resolution Radiometer
BRDF	Bidirectional Reflectance Distribution Function
DAAC	Distributed Active Archive Center
DVD	Digital Video Disk
EMD	Empirical Mode Decomposition
GAC	Global Area Coverage
LAC	Local Area Coverage
GIMMS	Global Inventory Monitoring and Modeling Studies
GLCF	Global Land Cover Facility
GSFC	Goddard Space Flight Center
GVI	Global Vegetation Index
ICA	Independent Component Analysis
ISLSCP	International Satellite Land Surface Climatology Project
NASA	National Aeronautics and Space Administration
NDVI	Normalized Difference Vegetation Index
NOAA	National Oceanographic and Atmospheric Administration
PAL	Pathfinder AVHRR Land
RMS	Root Mean Square Error
SR	Simple Ratio
SZA	Solar Zenith Angle